The effect of prefrontal stimulation on the firing of basal forebrain neurons in urethane anesthetized rat

Erika Gyengési[1,2], **Laszlo Zaborszky**[2], and **László Détári**[1]

1 *Eötvös Loránd University, Department of Physiology and Neurobiology, Budapest, H1117, Hungary*

2 *Rutgers University, Center for Molecular and Behavioral Neuroscience, Newark, NJ, 07102, USA*

Abstract

The basal forebrain (BF) contains a heterogeneous population of cholinergic and non-cholinergic corticopetal neurons and interneurons. Neurons firing at a higher rate during fast cortical EEG activity (f > 16Hz) were called F-cells, while neurons that increase their firing rate during high-amplitude slow-cortical waves (f < 4Hz) were categorized as S-cells. The prefrontal cortex (PFC) projects heavily to the BF, although little is know how it affects the firing of BF units. In this study, we investigated the effect of stimulation of the medial PFC on the firing rate of BF neurons (n=57) that were subsequently labeled by biocytin using juxtacellular filling (n=22). BF units were categorized in relation to tail-pinch induced and spontaneous EEG changes. Electrical stimulation of the medial PFC led to responses in 28 out of 41 F cells and in 8 out of 9 S cells. Within the sample of responsive F cells, 57% showed excitation (n=8) or excitation followed by inhibitory period (n=8). The remaining F cells expressed a short (n=6) or long inhibitory (n=6) response. In contrast, 75% of the recorded S cells (n=9) reduced their firing after prefrontal stimulation. Among the F-cells, we recovered one cholinergic neuron and one parvalbumin-containing neuron using juxtacellular filling and subsequent immunocytochemistry. While the PV cell displayed short latency facilitation, the cholinergic cell showed significant inhibition with much longer latency in response to the prefrontal stimulus. This is in agreement with previous anatomical data showing that prefrontal projections directly target mostly non-cholinergic cells, including GABAergic neurons.

Keywords

Cortical activation; Basal forebrain; Prefrontal cortex; Electrical stimulation; Juxtacellular labeling

1. Introduction

The basal forebrain (BF) is located at the medial and ventral part of the cerebral hemispheres. This area, including the medial septum, diagonal band nuclei, substantia innominata, pallidal (ventral pallidum, globus pallidus), and peripallidal regions, contains a heterogeneous population of neurons regarding their neurotransmitter content, morphology and projection pattern [1-4]. Among its cell populations, the cholinergic corticopetal projection neurons have received particular attention due to their loss or metabolic down regulation in Alzheimer's and related disorders [5-8]. Cholinergic neurons in the BF provide the major extrinsic source of

acetylcholine (ACh) to the cerebral cortex. Maximal release of ACh occurs in the cortex in association with cortical activation during states of waking and paradoxical sleep, suggesting that this projection is critically involved in the maintenance of cortical activation and in the process of normal wakefulness [9-11]. Cholinergic neurons are co-distributed with several other cell populations, including various calcium binding protein containing cells (e.g. calbindin, calretinin, parvalbumin), glutamatergic and GABAergic neurons [12-17]. Tracing studies using electron microscopy have identified synapses on BF neurons originating in the brainstem, hypothalamus, amygdala, substantia nigra-ventral tegmental area, striatum and the prefrontal cortex [2;16;18-23].

Experiments in animals, including primates [24;25], and human imaging studies [26-30] suggest the involvement of the prefrontal cortex (PFC) in higher cognitive functions, including planning, working memory and attention. Lesions in the BF, in experimental animals, resulted in attention deficits [31;32] and pharmacological manipulation in the PFC resulted in altered ACh efflux in posterior cortical areas [11;33-35], suggesting that a prefrontal-basalo-cortical circuitry may participate in the modulation of sensory processing.

Considerable amount of evidence has been accumulated on the functional heterogeneity of the PFC in rodents and primates [36]. The PFC is generally defined as that part of the frontal cortex that has reciprocal connection with the mediodorsal thalamic nucleus [37-40] and receives dense dopaminergic input from the ventral tegmental area [16;37;41-44]. In rodents, the PFC can be partitioned into medial, lateral and ventral or orbital subdivisions. The medial parts comprise the medial precentral area (Prc or M2), the anterior cingulate (Cg), the prelimbic (PL) and infralimbic areas (IL). The ventral areas encompass the medial, ventral, ventrolateral and lateral orbital areas, whereas the lateral subdivisions include the ventral and dorsal agranular insular areas. While the medial precentral and cingulate cortices project only with occasional fibers towards BF areas, the PL, IL and orbitofrontal areas give rise to relatively strong projections that pass through in a medio-lateral topography through BF areas rich in cholinergic neurons [19;45;46]. However, according to an electron microscopic study, prefrontal axons terminate exclusively on non-cholinergic neurons, including parvalbumin-containing cells [20].

In previous studies it has been revealed that the majority of BF neurons (so called F cells) have a strong positive correlation with EEG activity, meaning that cells showed an increased firing rate during low-voltage fast activity (LVFA, f > 16 Hz) in urethane anaesthetized rats. A smaller group of cells (S cells) also showed correlation with the changes in EEG, but in this case there was an increase in the firing rate during slow wave activity (SWA, f < 4 Hz) and they stopped or decreased their firing rate during LVFA [47-50]. In vivo extracellular recording with subsequent juxtacellular labeling and immunocytochemistry permitted further characterization of BF neurons [14;51;52]. Cholinergic neurons correspond to some of the F cells, however, according to our study, PV-containing, putative GABAergic neurons also belonged to the F category [51]. Among the S cells, several neurons containing NPY were found. In an effort to characterize the functional relationship between the PFC and BF areas we were interested to find out what is the functional effect of prefrontal stimulation on BF unit firing. Except one study, that investigated with electrophysiological methods the connection between the dorsomedial part of the PFC (Cg/M2) and BF [54], no data are available how more ventral parts of the PFC affect BF units. In this paper, we investigated the connection between BF and prefrontal areas using stimulation in PL/IL areas and recording single unit activity in the BF during EEG monitoring followed by juxtacellular labeling of the recorded neurons. Also, an attempt was made to immunohistochemically identify the juxtacellularly labeled cells. BF units were categorized in relation to tail-pinched induced and spontaneous EEG changes.

2. Experimental Procedure

Animal preparation

Experiments were performed on 31 Wistar male rats weighing 250-350 g. Animals were housed in temperature controlled environment and had free access to food and water. Animals were anesthetized with urethane (1.0-1.2 g/kg, i.p.), plus 4% lidocaine was injected at the cranial incision and ear canals. Supplementary doses of urethane (additional 10% of the original dosage) were also given when slow wave cortical activity appeared to be decreased. Animals showed no behavioral response to tail pinch during the experiment. Animals were fixed in a stereotaxic instrument (TSE Systems, Bad Hamburg, Germany). Square shaped holes were drilled according to the stereotaxic coordinates measured from the Bregma above BF areas. Body temperature was kept at 37 C by a heating pad (SuperTech, Pecs, Hungary). All surgical and animal care procedures adhered to the guidelines for the use and care of experimental animals of the European Communities Council Directive and the local Animal Care and Use Committee. All efforts were made to minimize animals' discomfort.

Electrode placement, electrophysiological recording and stimulation

Electrocortical activity (EEG) was recorded by a transcortical bipolar electrode (Teflon insulated stainless steel) (A: +2.0mm, L: 2.0 mm) through a small drilled hole on the right hemisphere. The superficial electrode touched the pial surface, while the deep one was reached 1.5 mm below the cortical surface. EEG was filtered between 0.1-100 Hz amplified and sampled at 200Hz. Following craniotomy single unit activity from BF neurons was recorded with glass capillary microelectrode (OD=2mm x ID=1.12, World Precision Instruments, Sarasota, FL, USA) pulled by a vertical puller (Narishige PE-2, Tokyo, Japan) resulted in a tip size 0.5-2μm. The electrode was filled up with 1.5-3% Biocytin (Sigma-Aldrich, Schelldorf, Germany) diluted in 0.5 M NaCl solution resulting in a tip resistance between 10-25MΩ. The electrode was positioned 1.4 mm posterior from the Bregma, 2.5-3 mm lateral and lowered 6 mm from the surface of the cortex after dura had been removed. Then advanced slowly (approximately 20-30 μm/min) using a piezo-electronic positioner (Burleigh 6000 ULN, Quebec, Canada). Unit activity was filtered between 300Hz-10 kHz and sampled at 30 kHz.

Prefrontal cortex (A: + 3.2mm, L: ± 0.5mm, D: 4mm) was stimulated with square-wave train pulses (A=0.5-1.5 mA; duration=0.3 msec; f=300Hz; n=3) delivered by a Grass stimulator (Grass Technologies, West Warwick, RI, USA) stimulator through a bipolar stimulating electrode (d=0.5 mm, stainless steel). The delay between two stimulations was about 3-5 sec in our experiments, though we randomized the process to avoid interference with the possible regular activity in the cortical EEG (slow cortical rhythm) and the unit activity.

Following a 5-minute baseline recording three series of 35 stimulus trains were given at different intensities (0.5-1.5 mA). After the stimulation was completed, an attempt was made to label the recorded neurons using the juxtacellular filling method described by Pinault [53]. The glass micropipette was carefully advanced closer to the neuron, and Biocytin was ejected by applying positive current pulses for 5-15 min (0.1-10 nA, 300 ms duration, 50% duty cycle) through the bridge circuit of the amplifier (Axoclamp - A2, Axon Instruments, Molecular Devices, Sunnyvale, CA, USA).

Perfusion, tissue processing and immunohistochemical staining

Rats were perfused transcardially with 50 ml PBS at room temperature followed by 400 ml cold 4% paraformaldehyde diluted in 0.1 M PBS (pH 7.4). The brain was removed from the skull and postfixed overnight in the same fixative at 4 C. The forebrain was cut by a Vibratome at 60μm thickness. Sections were collected from A: 0.5 to A: -2.5 mm from the Bregma. All histochemical procedures were performed using free-floating sections rinsed in 0.1 M PBS.

After cutting and rinsing, sections were incubated in Cy3 conjugated Streptavidin (1:500, Jackson Immuno Research, Suffolk, UK). The recorded and juxtacellularly filled neuron was found under an epiflourescence microscope (Olympus, BX51) and photographs were taken with a digital camera (FlouViewII Software) connected to the microscope. The labeled soma was processed for immunostaining for choline acetyltransferase (ChAT) and parvalbumin (PV) in the case of F cells, and neuropeptide-Y (NPY) and somatostatin (SS) in the case of S cells. To detect immunoreactivity the following antibodies were used: mouse anti-choline acetyltransferase monoclonal antibody (1:250, 1% Triton-X, Chemicon Int., Temecula, CA, USA) to visualize cholinergic cells followed by FITC- conjugated donkey anti - mouse IgG (1:300, Jackson Immuno Research); goat anti-parvalbumin (1:1000, 1% Triton-X, Swant, Bellinzona, Switzerland) followed by FITC- conjugated donkey anti - goat IgG (1:300, Jackson ImmunoResearch). Following incubation in the primary and secondary antibodies, sections were washed two times in PBS at room temperature then incubated in ABC (1:500, VectorLab, Burlingame, CA, USA) overnight at 4 C. They were then rinsed two times in PBS and once in Tris-buffer (TBS, pH 7.4) and then placed in TBS containing DAB (0.025%, Sigma-Aldrich), nickel sulfate (1%,) and ammonium chloride (1%) for 10-15 minutes. Reaction was stopped by extensive rinsing in PBS. Sections were then mounted onto gelatine-coated slides, dehydrated and cover slipped with DepEx (Serva, Heidelberg, Germany). If no cell bodies were found after Cy3 conjugated Streptavidine incubation, sections were mounted and Nissl-stained to visualize the electrode tracks.

Data analysis

Baseline spike trains (5-10 min) were analyzed (Spike and Origin 6.0 software) to obtain mean firing rate, to construct interspike interval histograms, and to test correlation between EEG waveforms and unit firing pattern. To determine characteristics of spike shapes, several spontaneous discharges were averaged using the same filtering conditions (300 Hz-10 kHz). Three qualities of spike shape have been calculated as described below. The width of the spikes was measured between the beginning of the first peak and the end of the first trough or the top of the second peak if there was any. The amplitude of the whole spike was calculated between the largest positive and negative values.

3. Results

Electrophysiology and PFC stimulation

A total of 57 neurons in the BF were studied, whereof 41 (72%) increased discharge rate when LVFA was present in the cortical EEG (F cells) and 9 (15%) showed increased firing rate during SWA. Also we found a group of cells (13%) that showed no correlation with any EEG pattern. We categorized neurons as F or S cells based on their response to tail pinch (TP) stimulation. Units were characterized as F cells if their activity increased due to TP stimulation, in contrast, the activity of S cells decreased following TP stimulation (Fig. 1). F cells significantly increased their firing rate due to tail pinch from 5.5 Hz±4.07 Hz to 8.4±5.41 Hz ($p \leq 0,05$; n=41). In S cells, the average firing rate significantly decreased from 7.9± 1.5 Hz to 5.8±1.7 Hz ($p \leq 0.05$; n=9) (Fig. 4/B). The firing rates of those neurons that we did not categorized either F or S cells showed almost no changes at all (before TP=10.44±9.74 Hz; after TP=10.47±8.16 Hz; n=7). Firing rates were calculated during a period of 5 sec before and after TP stimulation.

After the inspection of the PFC stimulation sites we found that 47 out of 57 locations were in the IL area of the medial PFC while in 10 cases the electrode track was found in the PL area (Fig. 2). Stimulation effects showed no correlation with the exact position of the stimulating electrode. We found that 28 F and 8 S cells responded to PFC stimulation (Fig. 3). F and S cells could be further sorted considering their responses to PFC stimuli. The majority of the F

cells showed excitation (F/+; n=8) and then returned to the level of their original activity, another group of cells (F+/-) showed massive positive response followed by a long inhibited period (n=8). In contrast, a smaller group of F cells (n=6) expressed a short negative, inhibitory response (F/-) while another 6 cells showed a long inhibition (F/--). In the case of S cells we found a group that showed inhibition (n=6) and a smaller, but clearly defined group (n=2) showing excitation in response to PFC stimuli. The average latency of excitatory responses, including F/+ and F+/- groups was 83.9± 28.1 ms. In the cases of inhibitory responses the latency was 110.7± 71.6 ms. Prestimulus firing rates during a 5-min period prior to PFC stimulation in these four groups of F cells showed significant differences compared to each other ($p \leq 0.05$): F/+ (0.85±0.31 Hz); F +/-(5.13±1.62 Hz); F/- (12.5±2.5 Hz); and F/-- (7.91±24 Hz). Because of the low number of S cells similar analysis was not performed.

EEG field potential—Pressure applied to the tail of the animal resulted in the activation of the EEG, however no motor response was observed. During the stimulation of the PFC, averaged evoked potentials in the M1/M2 area of the neocortex showed mostly similar shape and peaks (Fig. 3). These waves consisted of an early negative component, lasting up to 50 ms and a late, positive component, with duration of about 500ms. In many cases, firing of BF neurons increased and decreased closely following the positive and negative components of these evoked field potentials. When the negative component was correlated with increased unit activity in the BF, the positive component of the evoked potentials was expected to correlate with decreased BF neuronal activity. This alternation was a general pattern that has been observed regardless of cell types or responses given to prefrontal stimulus. Facilitation was always followed by inhibition in the activity of the BF units.

Juxtacellular labeling, localization and identification of the neurons

After PFC stimulation was completed, a total of 22 cells were successfully labeled with Biocytin. Biocytin positive neurons were distributed through the substantia innominata (SI) (n=12) and globus pallidus (GP) (n=9) or located at the border of the striatum (n=1). All of the biocytin labeled neurones were tested for immunohistochemical markers. In the case of F cells, we tried ChAT and PV, while in the cases of S cells, neurons were tested for SS and NPY. Two of these neurons were successfully identified by immunohistochemical methods: one contained ChAT, while the other PV (Fig. 5). The distribution of the F and S cells overlapped and no separation was found in respect to the different PFC stimulus responses either (Fig. 6). Of the Biocytin-labeled cells, 21 neurons matched the criteria of F cells and one neuron was classified as S cell based on the criteria described above. The PV cell was excited with short latency (10 ms) by the PFC stimulation. In contrast, long latency inhibition (100-300 ms) was seen in the case of the cholinergic neuron. In both identified cells, neuronal firing showed strong correlation with the changes of the field potential in the cortex and followed closely the PFC stimulus (Fig. 7).

Morphometry

After immunohistochemical analysis, sections were processed for NiDAB, to study juxtacellularly filled neurons under the light microscope: altogether 19 cells were recovered. The average diameter of the juxtacellularly filled neurons was 18.36±8.1 μm in horizontal and 17±4.7 μm in vertical directions. The vast majority of the cells were small to medium sized (10-25 μm in horizontal and vertical expansion) but 23% of the neurons were in the range of 25-35 μm. After measuring the horizontal and vertical diameters of each neuron we expressed the quotient of the values by dividing the larger value by the smaller one. Those cells in which the quotient was between 1.00 and 1.2 i.e. less than 20% difference were considered to be round, while a quotient larger than 1.2 meant ovoid neuron shape. Using Statistica 7 (StatSoft, Tulsa, OK, USA) software, we found 13 neurons to have ovoid cell body shape while 6 were categorized as having round shaped cell bodies. We applied a 2x2 contingency table to examine

the relationship between positive or negative responses to PFC stimulation and the shape of the soma. The chi square test was used to examine if the shape of the cell bodies and the response given to a stimulus was obtained by chance alone. We found that ovoid shaped neurons gave significantly more positive responses, while round shaped neurons were more frequently inhibited following PFC stimulus than expected (degree of freedom = 1; chi-square = 4.38; p = 0.0363).

We also tested if there is any correlation between spike shape and neuronal geometry. Spike width in ovoid shaped neurons (1.69 ± 0.42 ms, mean$\pm$SD), was less than in round shaped ones 1.9 ± 0.44 msec ($p \leq 0.05$). Peak-to-peak amplitude of spikes generated by ovoid shaped cells were significantly bigger (219 ± 80 µV) compared to the round shaped cells (142 ± 33 µV, $p \leq 0.05$).

3. Discussion

The present results confirm previous findings regarding the firing pattern and correlation of BF unit activity to cortical EEG [20;47-50]. Activity in the majority of the recorded neurons (50/57) changed in close correlation with cortical EEG. The unit activity of F cells (41/50) was strongly correlated to LVFA while S cells (9/50) remained silent or decreased their firing rate during fast EEG epochs. Stimulation of the medial prefrontal cortex affected 28 F and 8 S cells evoking diverse responses. In slightly less than half of the responding F cells (12/28) inhibition was the primary response, while the rest of the neurons were excited. In half of these cases, excitation was followed by inhibition. Those neurons that showed inhibition as a primary response differed further by the duration of their responses, which was either short (around 50 ms) or long (up to 300 ms). Most of the S cells (6/8) were inhibited by the PFC stimulation, but we also found two neurons that showed excitatory responses. It has already been proposed that the group of F cells show a higher degree of diversity than the S cells which is in agreement with our results from PFC stimulation as well.

Prefrontal-Basal Forebrain Connections

The medial PFC in both rats and primates gives rise to an important excitatory input to extensive BF regions in which cholinergic neurons are located [20;46], though prefrontal axons exclusively synapse on non-cholinergic neurons, at least in rats [20]. Despite of the excitatory nature of the projection, a large proportion of primary inhibitory responses were observed following PFC stimulation. This fact suggests that part of the cortical input could be relayed by inhibitory interneurons. The participation of interneurons is further supported by the long latencies observed in most of the responses (30-150 ms). The BF contains numerous GABAergic neurons [54] that co-localize different neuropeptides (NPY, SS, etc.) [20]. NPY and SS containing axon terminals were found to reach or even surround cholinergic cells [51;55]. It is not known yet whether these inhibitory neurons receive prefrontal input, but they would be good candidates to induce the observed inhibitions following PFC stimulation. A subgroup of these cells most likely consisted of interneurons and was probably hidden from the recording electrode due to the sampling bias of the method toward larger projection neurons. It is also known that PV containing, probably GABAergic neurons receive PFC input [20], hence they also may contribute to inhibitory responses evoked by PFC stimulation in BF neurons. Disfacilitation could provide another possible explanation for the inhibitory responses. Inhibition, or a decrease in activity in local neuronal networks of the mPFC as a consequence of the applied stimuli would indeed reduce the excitatory drive in the BF [56].

At last, nucleus accumbens is an important target of descending prefrontal fibers [57]. GABAergic cells of this striatal structure in turn, innervate cholinergic BF neurons [22]. As cortical input is excitatory, activation could be evoked through direct connections in non-cholinergic BF neurons or through antidromic invasion of the corticopetal neurons. However,

indirect pathways, through excitatory interneurons or by disinhibition could be also responsible for the excitatory responses. The neuronal pathways between the PFC and the locus coeruleus (LC) could also provide a possible explanation of the long latency responses. The noradrenergic LC recieves a potent excitatory mPFC input. In turn, it projects to the BF area including the substantia innominata [58;59].

The possibility of the antidromic activation was excluded because the neuronal responses did not meet even the two basic criteria of antidromic invasion: constant latency and high frequency following. Latencies of the excitatory responses were also relatively long, thus in most cases the indirect connection seems to be more probable.

In a previous paper, Golmayo et al.[60] found mostly short-latency (15-20 ms) excitatory responses in BF neurons following stimulation of the prefrontal cortex. These findings seem to contradict to our results. However, we observed in the present experiments that stimulation effects depended on the baseline activity in BF neurons. Those neurons that displayed a primary inhibitory response had a significantly higher firing rate than those cells, in which the response started with excitation. Based on their figures, baseline activity of BF cells were very low in the experiments reported by Golmayo et al. The depression of firing might have been caused by a deeper level of anesthesia than in our experiments as firing rate has been shown to continuously decrease with the deepening of anesthesia [49]. The exact explanation of the dependency of responses on baseline activity levels is not known, but similar observations were made earlier by Detari et al. [50]. Higher baseline firing rate predestined BF neurons to give smaller excitatory, or even inhibitory responses to short train stimulation of brainstem cholinergic (pedunculopontine) and serotoninergic (dorsal raphe) nuclei that was strongly excitatory at a low background firing rate. PPT effect on cholinergic BF neurons has been shown to be relayed by glutamatergic mechanisms, as cortical ACh release after PPT stimulation was blocked by BF injection of the nonspecific glutamatergic antagonist kynurenate acid, but not by scopolamine [10]. It can be suggested that glutamatergic input from the PFC reached local inhibitory interneurons (such as NPY and SS), PV containing projection neurons and possibly local excitatory interneurons (VGlut2) as well. It has been reported that VGlut2 is present in BF area [17], also a large population of VGlut2-immunoreactive neurons are located primarily in the posterior division of the septum [61]. A similar mechanism might explain the dependency of results of PFC stimuli on the background activity, observed in the present experiments.

F cells include cholinergic and PV-containing, supposedly GABAergic neurons. Using juxtacellular filling, we identified one cholinergic and one parvalbumin-containing F cell. Latency data measured in these cells were in good agreement with the fact that PFC input terminates on non-cholinergic neurons [20], as in the PV-containing neuron a short latency (10 ms) excitatory response was seen, while the cholinergic cell was inhibited with a latency of about 100 ms. Electrical stimulation of the prefrontal cortex or activation of glutamatergic and cholinergic receptors led to increased ACh release in neocortical areas [9;11]. These findings seem to contradict to the inhibitory response induced by PFC stimulation in the identified cholinergic cell in our experiments. However, our stimulation consisted of a short train of three stimuli inducing no generalized changes in EEG, while in the above cited papers more sustained stimulation was applied that led to LVFA in the cortical EEG. The exact mechanism by which sustained stimulation caused activation of BF cholinergic cells is not known, but it should occur through indirect, polysynaptic pathways as cholinergic cells receive no direct innervations from the PFC.

Prefrontal-Basal Forebrain-Cortical Loop

Vanderwolf et al. [62] in freely moving animals found cortical evoked responses following electrical stimulation of the contralateral sensorimotor cortex that were very similar to what

we have described in our experiments. Despite the similar sequence of negative and positive curves, durations were considerably longer and amplitudes smaller in our recordings. This finding could be explained by the use of urethane as anesthesia that, in general, tends to damp all kinds of activity in the neocortex, in particular those depending on multisynaptic pathways [63]. Evoked field potentials in the M1/M2 area displayed strong correlation with unit activity changes in the BF following PFC stimulation. Field potential changes started with a sharp wave (50 ms), negative at the deep layers of the cortex, thus indicating activation. This wave was followed by a longer positive wave (500 ms). This sequence was often followed by a second, slower negative wave. Previous studies suggested that the early component represents summed excitatory postsynaptic potentials; and the late component summed inhibitory postsynaptic potentials [62]. Not all components were always present in the neuronal responses; however latency and duration of excitatory and inhibitory periods ran parallel with field potential waves. An explanation for the very similar time course of the responses would be an excitation-inhibition-excitation sequence induced by the stimulus in the PFC itself. This activity pattern would then reach the neocortical areas and the BF separately and would ensure the similar timing of events. However, no important intercortical connection has been described between the mPFC and the M1/M2 areas either anatomically or electrophysiologically [39;45;46]. Therefore, it is highly unlikely that this strong correlation between the BF and M1/M2 areas can be explained by this mechanism. In contrast, it is well known that the BF provides a topographically organized projection to the whole cortical mantle [64] thus it is a more reasonable suggestion that BF neuronal changes were primary, evoked by the top-down projection from the PFC to the BF. Corticopetal projections from the BF would then induce the cortical responses. Similarly strong correlation has been reported between spontaneous neuronal activity in the BF and the cortical EEG and was explained by the bottom-up effects ascending from the BF to the cortex [49]. This observation could also give further support for the existence of the prefronto-basalo-cortical circuitry that has been already suggested [20].

Morphology

Several studies revealed the correlation between neuronal morphology and electrophysiological properties in different brain areas [65-67], while others claimed that no reliable physiological criteria could have been defined to distinguish certain neurotransmitter groups [68;69]. Spike shapes have been showed to carry specific neuronal information in cortical networks [70;71]. Morphological and electrophysiological characteristics of magnocellular neurons from basal forebrain nuclei of postnatal rats have been described in cell cultures. Four morphological subtypes of magnocellular neurons could be distinguished according to the shape of their soma and pattern of dendritic branching. Results from these experiments showed that, although acetyl cholinesterase-positive magnocellular basal forebrain neurons exhibit considerable morphological heterogeneity, they have very similar and characteristic electrophysiological properties [67]. Although, due to the small number of histochemicaly identified neurons, we could not conclude a correlation between certain electrophysiological properties - such as spike shape or response for a given stimulus - and neurotransmitter content. However, our findings showed a significant correlation between spike shape and response to PFC stimulus and neuronal soma shape suggesting that most likely by having higher number of identified neurons we might be able establish such criteria that would allow us to reliably classify neurons after careful electrophysiological analysis.

Concluding remarks—The electrophysiological diversity of the recorded neurons based on their spontaneous activity and responses to the PFC stimulation reflects the existence of different BF cell types that receive direct or indirect prefrontal input. Unfortunately, we were able to identify only very few neurons chemically, preventing us to establish whether or not the different electrophysiological categories correspond to different cell types or different functional states. The observation, however, in case of similar firing rates of S and F cells, that

BF neurons display different behavior in response to ascending (tail pinch) or descending (prefrontal) stimuli suggest that the prevalent state of activity of neurons may be important in determining their responses.

Acknowledgements

Reference List

1. Alheid GF. Extended amygdala and basal forebrain. Ann N Y Acad Sci 2003;985:185–205. [PubMed: 12724159]

2. Zaborszky L. Afferent connections of the forebrain cholinergic projection neurons, with special reference to monoaminergic and peptidergic fibers. EXS 1989;57:12–32. [PubMed: 2533086]

3. Zaborszky L. The modular organization of brain systems. Basal forebrain: the last frontier. Prog Brain Res 2002;136:359–372. [PubMed: 12143394]

4. Zaborszky L, Buhl DL, Pobalashingham S, Bjaalie JG, Nadasdy Z. Three-dimensional chemoarchitecture of the basal forebrain: spatially specific association of cholinergic and calcium binding protein-containing neurons. Neuroscience 2005;136:697–713. [PubMed: 16344145]

5. Averback P. Lesions of the nucleus ansae peduncularis in neuropsychiatric disease. Arch Neurol 1981;38:230–235. [PubMed: 6452111]

6. Geula, C.; Mesulam, MM. Cholinergic systems and related neuropathological predilection patterns in Alzheimer Disease. Raven Press; New York: 1994. p. 263-291.

7. Jellinger, K. Advances in neurology. Plenum Press; New York: 1996. New developments in the pathology of Parkinson's disease; p. 1-6.

8. Perry EK. Cholinergic transmitter and neurotrophic activities in Lewy body dementia: similarity to Parkinson's and distinction from Alzheimer disease. Alzheimer Dis assoc Disord. 1993

9. Dringenberg HC, Vanderwolf CH. Neocortical activation: modulation by multiple pathways acting on central cholinergic and serotonergic systems. Exp Brain Res 1997;116:160–174. [PubMed: 9305825]

10. Rasmusson DD, Clow K, Szerb JC. Modification of neocortical acetylcholine release and electroencephalogram desynchronization due to brainstem stimulation by drugs applied to the basal forebrain. Neuroscience 1994;60:665–677. [PubMed: 7936193]

11. Sarter M, Parikh V. Choline transporters, cholinergic transmission and cognition. Nat Rev Neurosci 2005;6:48–56. [PubMed: 15611726]

12. Manns ID, Alonso A, Jones BE. Rhythmically discharging basal forebrain units comprise cholinergic GABAergic, and putative glutamatergic cells. J Neurophysiol 2003;89:1057–1066. [PubMed: 12574480]

13. Manns ID, Mainville L, Jones BE. Evidence for glutamate in addition to acetylcholine, GABA, neurotransmitter synthesis in basal forebrain neurons projecting to the entorhinal cortex. Neuroscience 2001;107:249–263. [PubMed: 11731099]

14. Manns ID, Alonso A, Jones BE. Discharge profiles of juxtacellularly labeled and immunohistochemically identified GABAergic basal forebrain neurons recorded in association with the electroencephalogram in anesthetized rats. J Neurosci 2000;20:9252–9263. [PubMed: 11125003]

15. Ribak CE, Roberts RC. GABAergic synapses in the brain identified with antisera to GABA its synthesizing enzyme, glutamate decarboxylase. J Electron Microsc Tech 1990;15:34–48. [PubMed: 2187069]

16. Gaykema RP, Zaborszky L. Parvalbumin-containing neurons in the basal forebrain receive direct input from the substantia nigra-ventral tegmental area. Brain Res 1997;747:173–179. [PubMed: 9042545]

17. Hur EE, Zaborszky L. Vglut2 afferents to the medial prefrontal and primary somatosensory cortices: a combined retrograde tracing in situ hybridization. J Comp Neurol 2005;483:351–373. [PubMed: 15682395]

18. Cullinan WE, Zaborszky L. Organization of ascending hypothalamic projections to the rostral forebrain with special reference to the innervation of cholinergic projection neurons. J Comp Neurol 1991;306:631–667. [PubMed: 2071698]

19. Gaykema RP, van Weeghel R, Hersh LB, Luiten PG. Prefrontal cortical projections to the cholinergic neurons in the basal forebrain. J Comp Neurol 1991;303:563–583. [PubMed: 2013647]

20. Zaborszky L, Gaykema RP, Swanson DJ, Cullinan WE. Cortical input to the basal forebrain. Neuroscience 1997;79:1051–1078. [PubMed: 9219967]

21. Zaborszky L, Cullinan WE. Direct catecholaminergic-cholinergic interactions in the basal forebrain. I. Dopamine-beta-hydroxylase- and tyrosine hydroxylase input to cholinergic neurons. J Comp Neurol 1996;374:535–554. [PubMed: 8910734]

22. Zaborszky L, Cullinan WE. Projections from the nucleus accumbens to cholinergic neurons of the ventral pallidum: a correlated light and electron microscopic double-immunolabeling study in rat. Brain Res 1992;570:92–101. [PubMed: 1617433]

23. Zaborszky L, Leranth C, Heimer L. Ultrastructural evidence of amygdalofugal axons terminating on cholinergic cells of the rostral forebrain. Neurosci Lett 1984;52:219–225. [PubMed: 6521966]

24. Chiba AA, Bucci DJ, Holland PC, Gallagher M. Basal forebrain cholinergic lesions disrupt increments but not decrements in conditioned stimulus processing. J Neurosci 1995;15:7315–7322. [PubMed: 7472485]

25. Sarter M, Hasselmo ME, Bruno JP, Givens B. Unraveling the attentional functions of cortical cholinergic inputs: interactions between signal-driven and cognitive modulation of signal detection. Brain Res Brain Res Rev 2005;48:98–111. [PubMed: 15708630]

26. Breiter HC, Rosen BR. Functional magnetic resonance imaging of brain reward circuitry in the human. Ann N Y Acad Sci 1999;877:523–547. [PubMed: 10415669]

27. Maquet P, Franck G. REM sleep and amygdala. Mol Psychiatry 1997;2:195–196. [PubMed: 9152982]

28. Maquet P, Degueldre C, Delfiore G, Aerts J, Peters JM, Luxen A, Franck G. Functional neuroanatomy of human slow wave sleep. J Neurosci 1997;17:2807–2812. [PubMed: 9092602]

29. Morris NP, Harris SJ, Henderson Z. Parvalbumin-immunoreactive, fast-spiking neurons in the medial septum/diagonal band complex of the rat: intracellular recordings in vitro. Neuroscience 1999;92:589–600. [PubMed: 10408608]

30. Paus T, Zatorre RJ, Hofle N, Caramanos Z, Gotman J, Petrides M, Evans AC. Time-related changes in neural systems underlying attention and arousal during the performance of an auditory vigilance task. J Cogn Neurosci 1997;9:392–408.

31. Voytko ML, Olton DS, Richardson RT, Gorman LK, Tobin JR, Price DL. Basal forebrain lesions in monkeys disrupt attention but not learning and memory. J Neurosci 1994;14:167–186. [PubMed: 8283232]

32. Wang Y, Nakashima K, Shiraishi Y, Kawai Y, Ohama E, Takahashi K. P300-like potential disappears in rabbits with lesions in the nucleus basalis of Meynert. Exp Brain Res 1997;114:288–292. [PubMed: 9166918]

33. Rasmusson D, Szerb JC. Acetylcholine release from visual and sensorimotor cortices of conditioned rabbits: the effects of sensory cuing and patterns of responding. Brain Res 1976;104:243–259. [PubMed: 1260422]

34. Rasmusson D, Szerb JC. Cortical acetylcholine release during operant behaviour in rabbits. Life Sci 1975;16:683–690. [PubMed: 1123966]

35. Sarter M, Nelson CL, Bruno JP. Cortical cholinergic transmission and cortical information processing in schizophrenia. Schizophr Bull 2005;31:117–138. [PubMed: 15888431]

36. Robbins TW. Chemistry of the mind: neurochemical modulation of prefrontal cortical function. J Comp Neurol 2005;493:140–146. [PubMed: 16254988]

37. Gabbott PL, Warner TA, Jays PR, Salway P, Busby SJ. Prefrontal cortex in the rat: projections to subcortical autonomic motor, and limbic centers. J Comp Neurol 2005;492:145–177. [PubMed: 16196030]

38. Uylings HB, Groenewegen HJ, Kolb B. Do rats have a prefrontal cortex? Behav Brain Res 2003;146:3–17. [PubMed: 14643455]

39. Vertes RP. Differential projections of the infralimbic and prelimbic cortex in the rat. Synapse 2004;51:32–58. [PubMed: 14579424]

40. Wang CC, Shyu BC. Differential projections from the mediodorsal and centrolateral thalamic nuclei to the frontal cortex in rats. Brain Res 2004;995:226–235. [PubMed: 14672812]

41. Franke H, Schelhorn N, Illes P. Dopaminergic neurons develop axonal projections to their target areas in organotypic co-cultures of the ventral mesencephalon and the striatum/prefrontal cortex. Neurochem Int 2003;42:431–439. [PubMed: 12510026]

42. Gaykema RP, Zaborszky L. Direct catecholaminergic-cholinergic interactions in the basal forebrain. II. Substantia nigra-ventral tegmental area projections to cholinergic neurons. J Comp Neurol 1996;374:555–577. [PubMed: 8910735]

43. Reynolds SM, Zahm DS. Specificity in the projections of prefrontal and insular cortex to ventral striatopallidum and the extended amygdala. J Neurosci 2005;25:11757–11767. [PubMed: 16354934]

44. Sesack SR, Bunney BS. Pharmacology of Dopamine-Induced Electrophysiological Responses in the Rat Prefrontal Cortex - D1-Mediated Or D2-Mediated. Annals of the New York Academy of Sciences 1988;537:529–530.

45. Hurley KM, Herbert H, Moga MM, Saper CB. Efferent projections of the infralimbic cortex of the rat. J Comp Neurol 1991;308:249–276. [PubMed: 1716270]

46. Sesack SR, Deutch AY, Roth RH, Bunney BS. Topographical organization of the efferent projections of the medial prefrontal cortex in the rat: an anterograde tract-tracing study with Phaseolus vulgaris leucoagglutinin. J Comp Neurol 1989;290:213–242. [PubMed: 2592611]

47. Detari L. Tonic and phasic influence of basal forebrain unit activity on the cortical EEG. Behav Brain Res 2000;115:159–170. [PubMed: 11000418]

48. Detari L, Rasmusson DD, Semba K. The role of basal forebrain neurons in tonic and phasic activation of the cerebral cortex. Prog Neurobiol 1999;58:249–277. [PubMed: 10341363]

49. Detari L, Rasmusson DD, Semba K. Phasic relationship between the activity of basal forebrain neurons and cortical EEG in urethane-anesthetized rat. Brain Res 1997;759:112–121. [PubMed: 9219869]

50. Detari L, Semba K, Rasmusson DD. Responses of cortical EEG-related basal forebrain neurons to brainstem and sensory stimulation in urethane-anaesthetized rats. Eur J Neurosci 1997;9:1153–1161. [PubMed: 9215698]

51. Duque A, Balatoni B, Detari L, Zaborszky L. EEG correlation of the discharge properties of identified neurons in the basal forebrain. J Neurophysiol 2000;84:1627–1635. [PubMed: 10980032]

52. Manns ID, Alonso A, Jones BE. Discharge properties of juxtacellularly labeled and immunohistochemically identified cholinergic basal forebrain neurons recorded in association with the electroencephalogram in anesthetized rats. J Neurosci 2000;20:1505–1518. [PubMed: 10662840]

53. Pinault D. A novel single-cell staining procedure performed in vivo under electrophysiological control: morpho-functional features of juxtacellularly labeled thalamic cells and other central neurons with biocytin or Neurobiotin. J Neurosci Methods 1996;65:113–136. [PubMed: 8740589]

54. Gritti I, Mainville L, Jones BE. Projections of GABAergic and cholinergic basal forebrain and GABAergic preoptic-anterior hypothalamic neurons to the posterior lateral hypothalamus of the rat. J Comp Neurol 1994;339:251–268. [PubMed: 8300907]

55. Zaborszky L, Duque A. Local synaptic connections of basal forebrain neurons. Behav Brain Res 2000;115:143–158. [PubMed: 11000417]

56. Wilson CJ, Chang HT, Kitai ST. Disfacilitation and long-lasting inhibition of neostriatal neurons in the rat. Exp Brain Res 1983;51:227–235. [PubMed: 6194008]

57. Gorelova N, Yang CR. The course of neural projection from the prefrontal cortex to the nucleus accumbens in the rat. Neuroscience 1997;76:689–706. [PubMed: 9135043]

58. Jodo E, Chiang C, Aston-Jones G. Potent excitatory influence of prefrontal cortex activity on noradrenergic locus coeruleus neurons. Neuroscience 1998;83:63–79. [PubMed: 9466399]

59. Espana RA, Berridge CW. Organization of noradrenergic efferents to arousal-related basal forebrain structures. J Comp Neurol 2006;496:668–683. [PubMed: 16615125]

60. Golmayo L, Nunez A, Zaborszky L. Electrophysiological evidence for the existence of a posterior cortical-prefrontal-basal forebrain circuitry in modulating sensory responses in visual and somatosensory rat cortical areas. Neuroscience 2003;119:597–609. [PubMed: 12770572]

61. Hajszan T, Alreja M, Leranth C. Intrinsic vesicular glutamate transporter 2-immunoreactive input to septohippocampal parvalbumin-containing neurons: novel glutamatergic local circuit cells. Hippocampus 2004;14:499–509. [PubMed: 15224985]

62. Vanderwolf CH, Harvey GC, Leung LW. Transcallosal evoked potentials in relation to behavior in the rat: effects of atropine p-chlorophenylalanine reserpine, scopolamine and trifluoperazine. Behav Brain Res 1987;25:31–48. [PubMed: 2956970]

63. Bindmann, LJ.; Lippold, O. The Neurophysiology of the Cerebral Cortex. London: Edward Arnold Ltd; 1981.

64. Zaborszky L, Pang K, Somogyi J, Nadasdy Z, Kallo I. The basal forebrain corticopetal system revisited. Ann N Y Acad Sci 1999;877:339–367. [PubMed: 10415658]

65. Uusisaari M, Obata K, Knopfel T. Morphological and electrophysiological properties of GABAergic and non-GABAergic cells in the deep cerebellar nuclei. J Neurophysiol 2007;97:901–911. [PubMed: 17093116]

66. Washburn MS, Moises HC. Electrophysiological and morphological properties of rat basolateral amygdaloid neurons in vitro. J Neurosci 1992;12:4066–4079. [PubMed: 1403101]

67. Sim JA, Allen TG. Morphological and membrane properties of rat magnocellular basal forebrain neurons maintained in culture. J Neurophysiol 1998;80:1653–1669. [PubMed: 9772229]

68. Margolis EB, Lock H, Hjelmstad GO, Fields HL. The ventral tegmental area revisited: is there an electrophysiological marker for dopaminergic neurons? J Physiol 2006;577:907–924. [PubMed: 16959856]

69. Likhtik E, Pelletier JG, Popescu AT, Pare D. Identification of basolateral amygdala projection cells and interneurons using extracellular recordings. J Neurophysiol 2006;96:3257–3265. [PubMed: 17110739]

70. Juusola M, Robinson HP, de Polavieja GG. Coding with spike shapes and graded potentials in cortical networks. Bioessays 2007;29:178–187. [PubMed: 17226812]

71. de Polavieja GG, Harsch A, Kleppe I, Robinson HP, Juusola M. Stimulus history reliably shapes action potential waveforms of cortical neurons. J Neurosci 2005;25:5657–5665. [PubMed: 15944394]
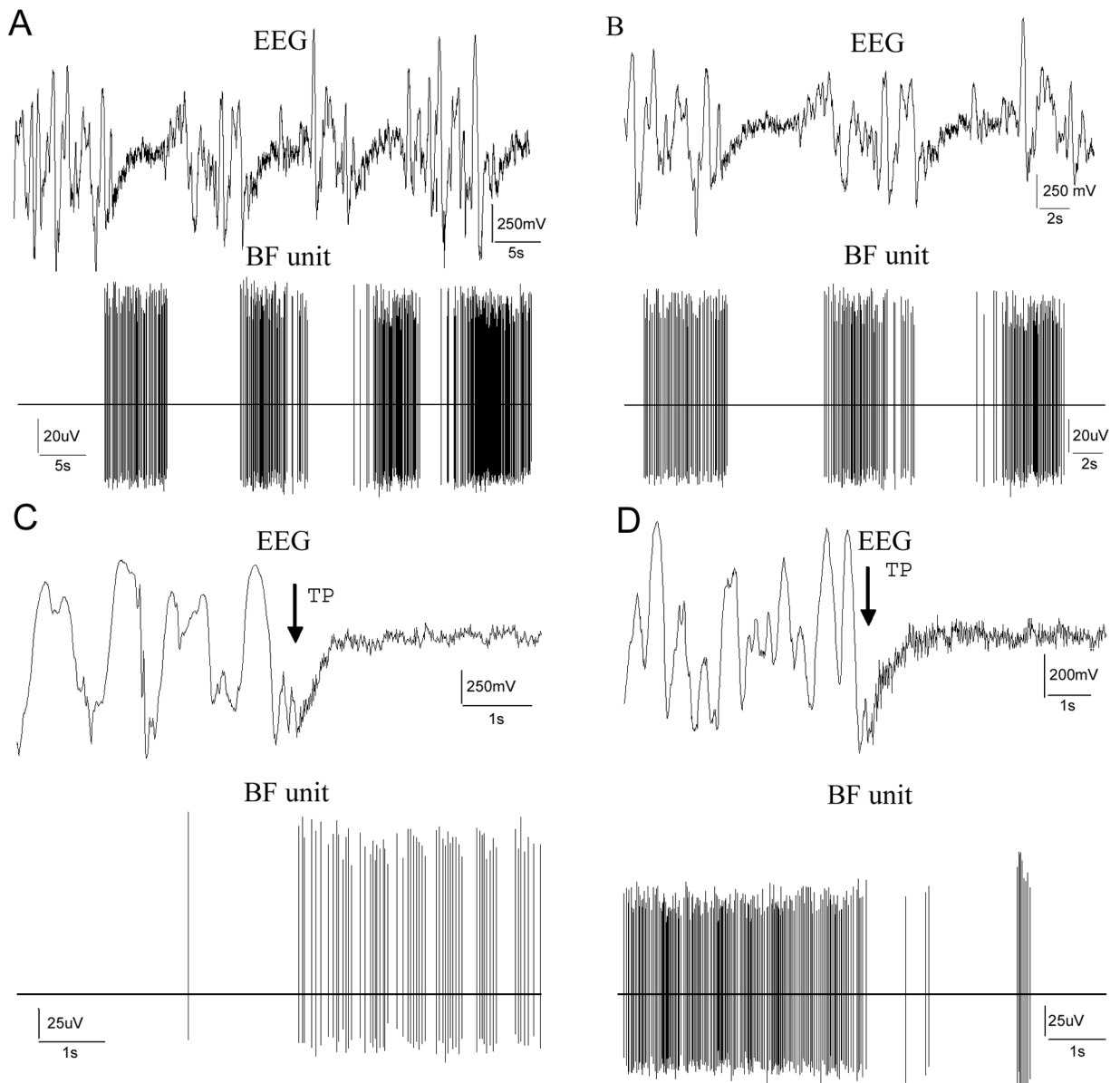
Fig. 1.
Properties of F and S cells in the BF. A,B) Raw data illustrating the spontaneous changes in the EEG and in the firing rate of an F and S cell, respectively. Spontaneous changes of cortical SWA to LVFA were followed by the increase or decrease of unit activity. C) Figure representing raw data from the recording of an F cell that increased its firing activity due to TP stimuli. D) An example of an S cells, that suspended its firing for a longer period of time in close correlation with cortical activation (bin width=10 ms).
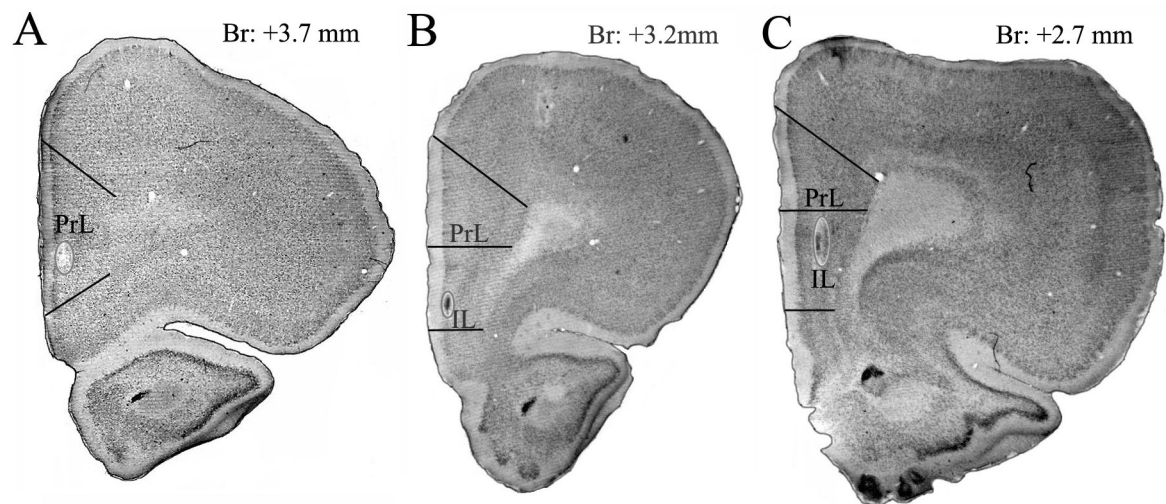
Fig 2.
Location of PFC stimulating electrodes. After histochemical procedures had been done, stimulating electrode tracks were located in the PFC. Stimulation sites have been detected from +3.7 mm to +2.7 mm anterior from the Bregma. Out of 57 stimulation sites, 47 were found in the infralimbic (IL) area, while in 10 cases, it was in the prelimbic (PrL) area.
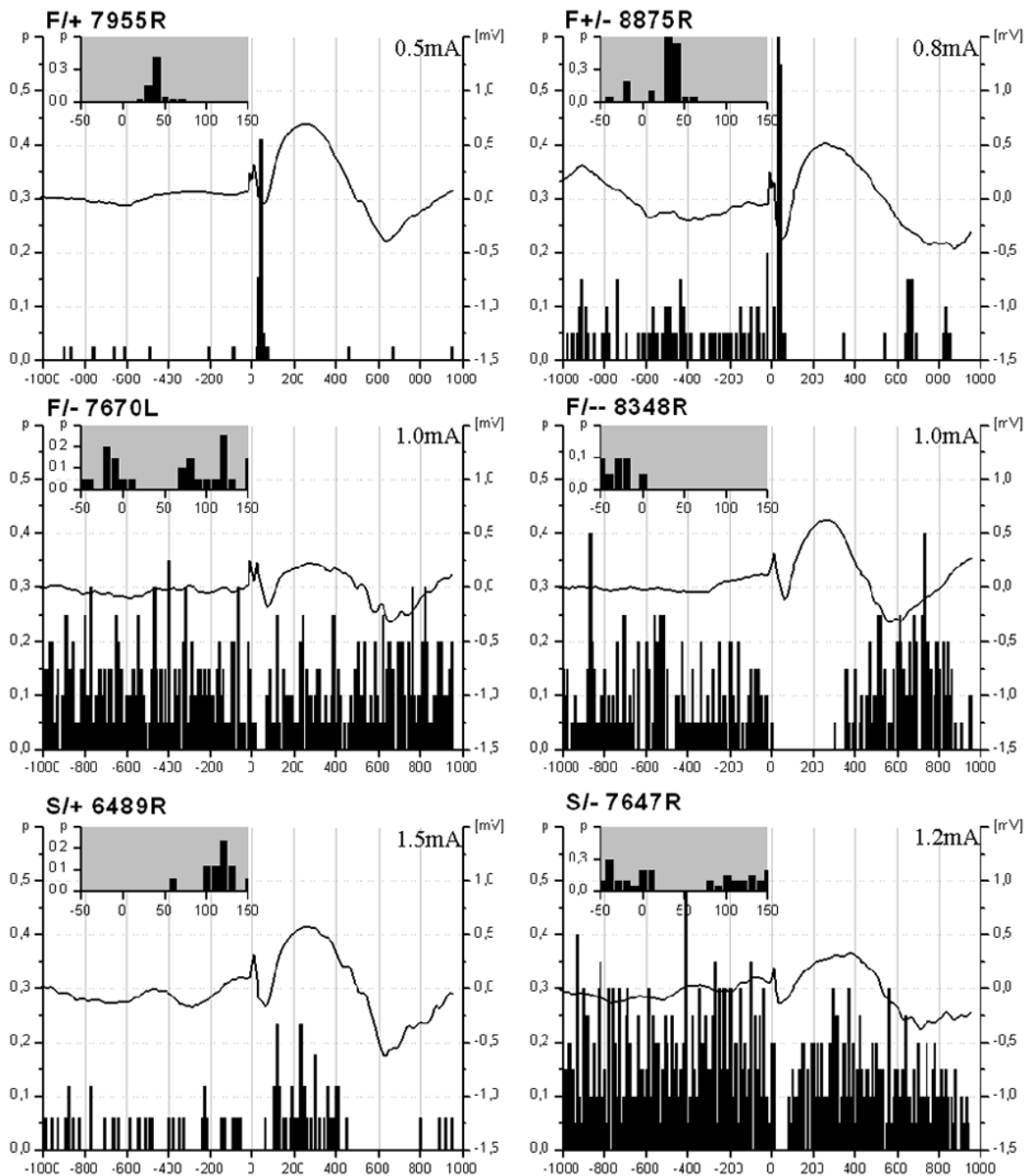
Fig. 3.
Diversity of changes in neuronal activity in F-, and S-cells following PFC stimulation. Both F and S cells showed inhibition or facilitation as a response for the PFC stimuli, though among F cells, a higher degree of diversity was found. Inhibitory responses were more frequent in neurons with higher background activity while facilitation occurred in those cases when the neurons showed relatively low discharge rate. Black curves show averaged cortical evoked potentials recorded from the M1/M2 cortical areas. Insets of the peri-event time histograms (PETHs) zoom in on the first 150 ms of the evoked responses.
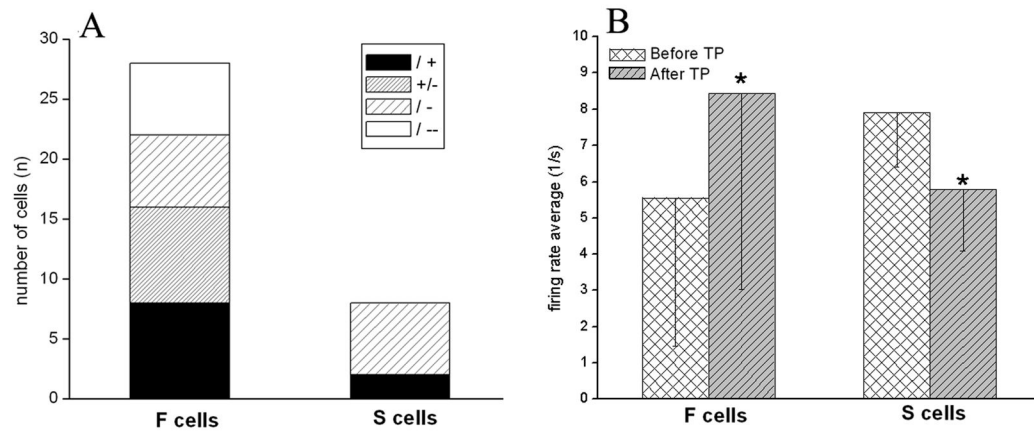
Fig. 4.
Graphic representation of the number of different categorized neurons (A) registered in the BF and the firing rates of F and S cells before and after TP stimulation (B). A) Out of 57 neurons we found 41 F cells and 9 S cells. B) This categorization was based on their firing rates before and after TP stimulation. The firing activity of F cells significantly increased (before TP=5.5 Hz; after TP=8.4 Hz; n=41), while S cells significantly decreased (before TP=7.9± 1.5 Hz; after TP=5.8±1.7 Hz; n=9) their firing rate due to TP (p<0.05).
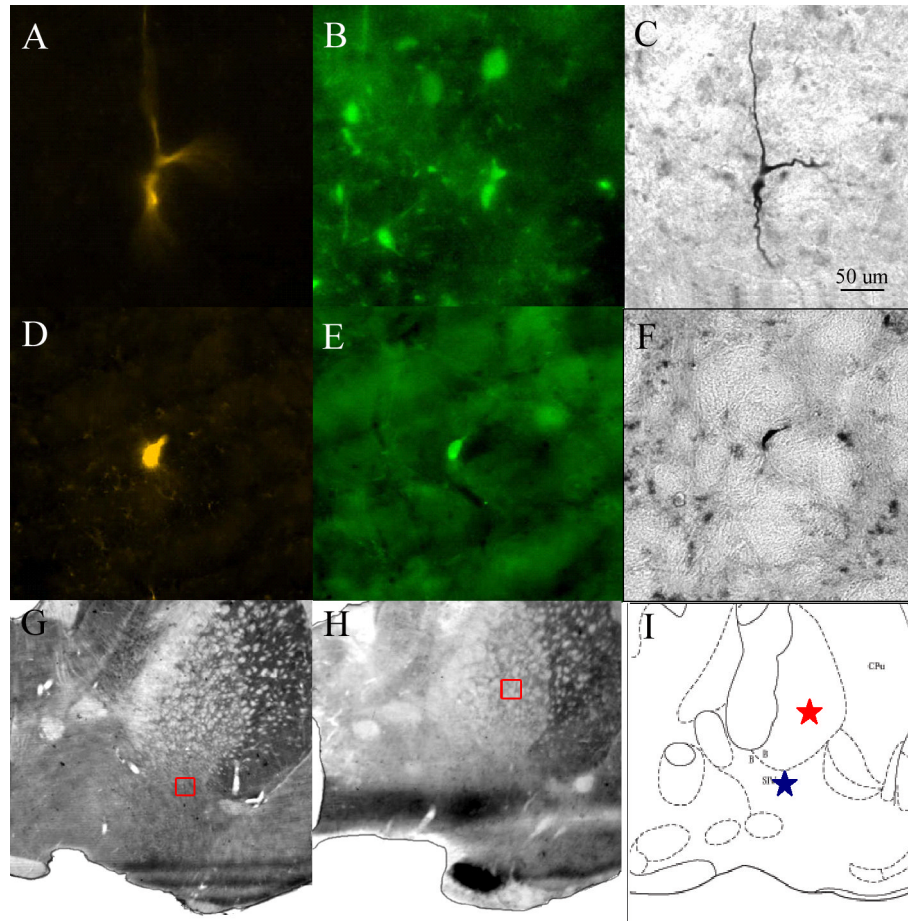
Fig 5.
Digital photographs of juxtacellularly labeled and identified PV-containing (first row A, B, C)
and cholinergic (D, E, F) neurons. A, D) Cy3-conjugated Streptavidine staining. B) FITC-
conjugated donkey anti - goat IgG to visualize Gt-anti-PV staining. E) FITC- conjugated
donkey anti - mouse IgG to visualize Ms-anti-ChAT staining. C, F) neurons developed with
Ni-DAB. G, H) Location of the PV-containing and cholinergic neurons, respectively, marked
by a small red square. I) Location of the two identified neurons on a schematic figure from rat
brain atlas. ★ represents the cholinergic neuron, while ★ stands for the parvalbumin containing
cell.
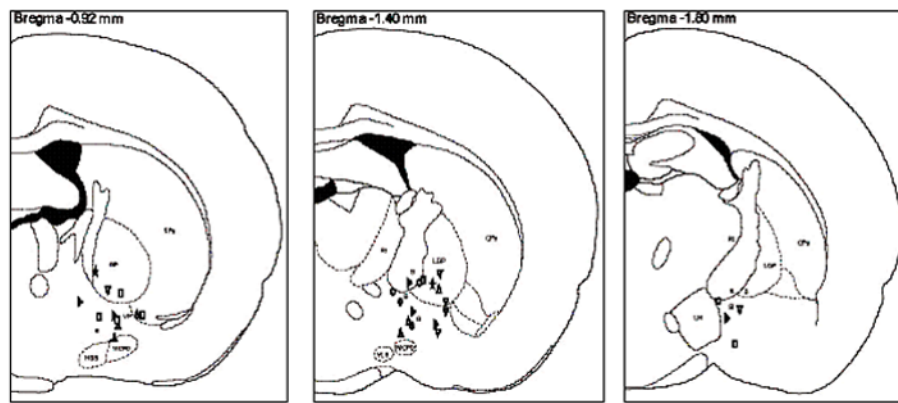
Fig. 6.
Distribution of the recorded neurons in the BF plotted on coronal sections from the Paxinos-Watson atlas. Most of the recorded neurons were located in the substantia innominata, the ventral pallidum and globus pallidus.
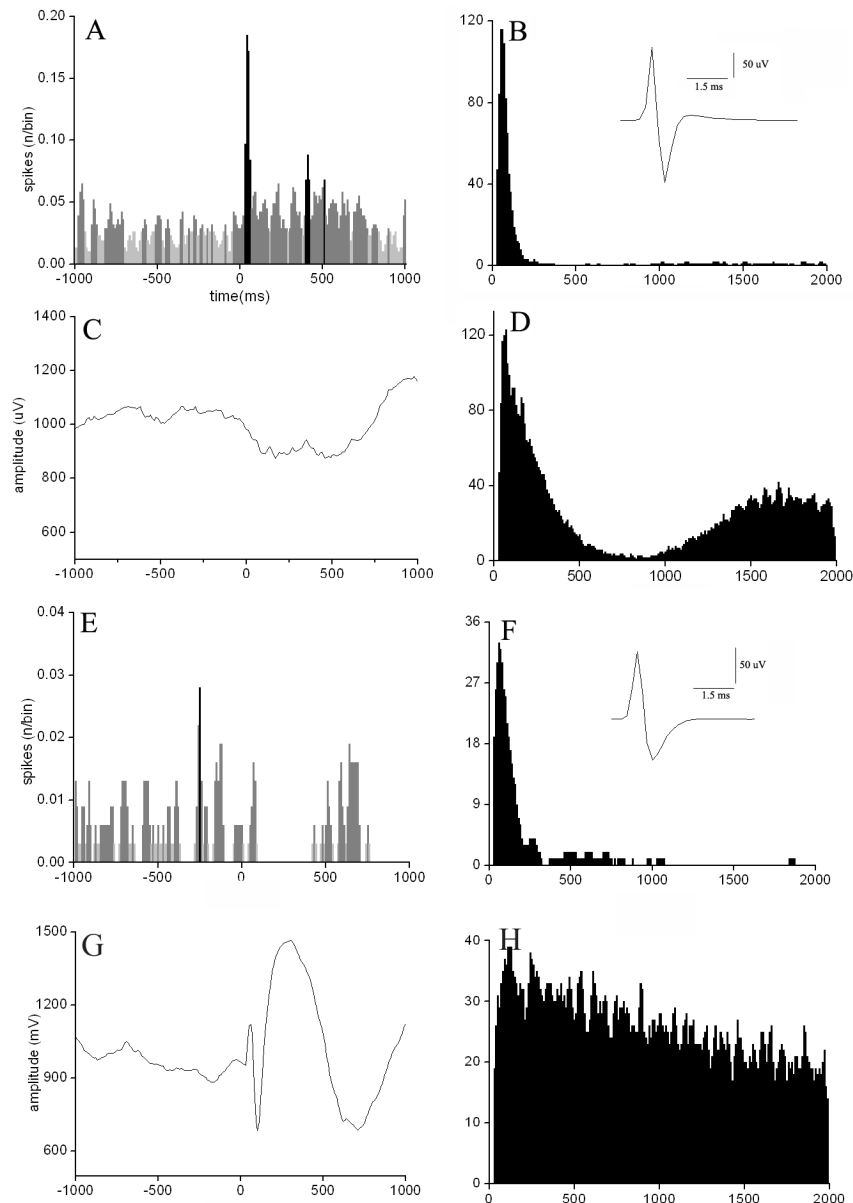
Fig 7.
Analysis of the identified parvalbumin (A-D) containing and cholinergic (E-H) neurons. A, C) shows the averaged response of the unity activity of the PV cell and the simultaneous EEG for PFC stimulus (intensity of stimulation: I=0.5 mA), that resulted in a positive peak in the unit activity E, G) demonstrates the same diagram in the case of the cholinergic neuron, in which case only a slight difference of the discharge activity has been determined compared to the baseline spike number/bin (1 bin=10ms) while using stimulation intensity of 35 mA. B, D) and F, H) show the interspike interval histogram (ISIH) and autocorrelogram of the unit activity of the PV and the cholinergic neuron, respectively. Insets in panels B and F illustrate the spike shapes of the neurons. We have found the spike width of the two neurons are approximately the same (0.8-2ms).